

Real-Time Testbed for Diversity in Powerline and Wireless Smart Grid Communications

Junmo Sung and Brian L. Evans

Wireless Networking and Communications Group

The University of Texas at Austin, Austin, Texas 78712 USA

Email: junmo.sung@utexas.edu, bevans@ece.utexas.edu

Abstract—Two-way communication is a key feature in a smart grid. It is enabled by either powerline communication or wireless communication technologies. Utilizing both technologies can potentially enhance communication reliability, and many diversity combining schemes have been proposed. In this paper, we propose a flexible real-time testbed to evaluate diversity combining schemes over physical channels. The testbed provides essential parts of physical layers on which both powerline and wireless communications operate. The contributions of this paper are 1) implementation of a real-time testbed for diversity of simultaneous powerline and wireless communications, and 2) performance evaluation of maximal ratio combining (MRC) on the testbed. Bit error rate curves obtained from simulations and measurements over physical channels show that performance of MRC in practice is comparable with simulation in various test cases.

I. INTRODUCTION

People living in modern society rely on electronic devices and appliances more than ever. Put differently, our society relies on electricity more than any other in human history. Power outages, thus, degrade the quality of life and cause damage to businesses. Power outages cost the U.S. more than \$100B per year [1], [2]. Furthermore aging infrastructure will make it challenging to meet the growing power demand. Replacing aging coal plants, which generate about one third of the electricity in the U.S. [3], will require an estimated \$560B by 2030. In 2015, 94 coal plants with an average age of 54 years were retired [4], which amounts to nearly 5% of total U.S. coal capacity. In traditional power grids, the unidirectional flow of information and electricity hinders precise demand prediction and integration of renewable and other energy sources.

Smart grids which have seen initial trials by several utilities [5], [6] are anticipated to be solutions for managing the growing demand by distributing energy in an unconventional and smart manner [7]–[9]. As an integration of communication and electricity distribution networks, information conveyed through the communication network is exploited to improve reliability and efficiency of the distribution system. Smart meters, thus, are expected to play a key role in smart grid

This work was supported by the Semiconductor Research Corporation (SRC) under SRC GRC Task ID 1836.133 with industry liaisons Texas Instruments and NXP Semiconductors through the Texas Analog Center of Excellence at The University of Texas at Dallas.

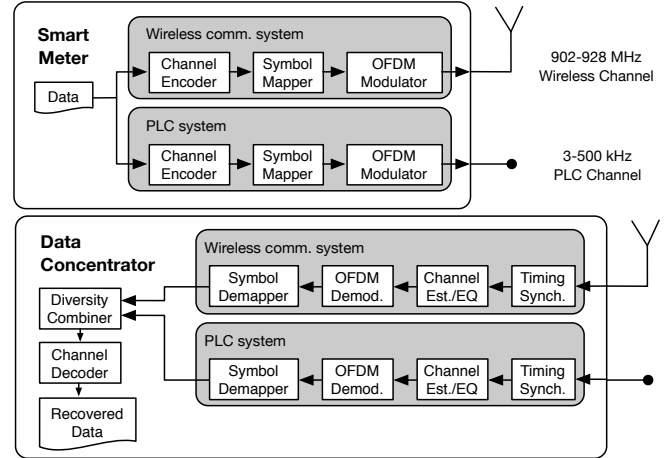


Fig. 1: Diagram of PLC/Wireless Diversity System

communication [10]. They are capable of not only measuring power consumption at users' end but also exchanging information such as measured data, meter status, and control commands between smart meters and a data concentrator.

This two-way communication is being enabled by either powerline communication (PLC) or wireless communication technologies. Power lines experience more complicated noise and interference, which result in modeling and mitigation techniques that are different from those for the wireless channels [11], [12]. Smart meters are designed to use either PLC or wireless communications or can switch between them, but do not make simultaneous use of both. One promising way to enhance communication reliability is to utilize the two independent communication technologies available for the smart grid [13]–[16]. Fig. 1 illustrates an overall diagram of a physical layer of a PLC and wireless diversity system. Theoretical studies show that diversity schemes help the network to become more reliable. Diversity combining schemes need to be implemented and tested in order to verify functionality and evaluate performance under realistic conditions.

Extensive surveys on smart grid testbeds were recently conducted [17], [18], and a variety of targeted research areas of the testbeds include cyber security, power grid management, energy efficiency and communications. To the best of authors' knowledge, however, there has not been such testbed

implementation that provides test environment for evaluation of diversity combining over the PLC and wireless communications. A flexible real-time testbed that we present in this paper is intended for such purposes. It provides essential parts of physical layers on which simultaneous over-the-wire and over-the-air smart grid communications operate. The contributions of this paper are: 1) we propose a flexible real-time testbed for evaluation of diversity combining schemes over simultaneous powerline and wireless communications and provide details of implementation as well as the code [19] and 2) we evaluate performance of maximal ratio combining (MRC), as an example, implemented in the real-time testbed. Bit error rate (BER) curves from both simulations and measurements are plotted and show that the performance of MRC in practice is comparable with simulation in various test cases.

II. POWERLINE AND WIRELESS COMMUNICATION DIVERSITY

Assuming a subcarrier bandwidth in orthogonal frequency division multiplexing (OFDM) is small enough compared to the coherence bandwidth of a channel, received symbols in each subcarrier, $Y_{n,k}$, can be expressed as

$$Y_{n,k}^p = H_{n,k}^p X_{n,k} + N_{n,k}^p \quad (1)$$

$$Y_{n,k}^w = H_{n,k}^w X_{n,k} + N_{n,k}^w \quad (2)$$

where $X_{n,k}$, $H_{n,k}$ and $N_{n,k}$ are the transmitted symbol, channel impulse response and additive noise in the frequency domain, respectively, at the k^{th} subcarrier in the n^{th} OFDM symbol, and $(\cdot)^p$ and $(\cdot)^w$ denote PLC and wireless links, respectively.

The two communication links can be exploited for higher data rate or better reliability in the smart grid. We apply diversity in the heterogeneous communications to combine two received symbols in order to improve reliability. Among combining schemes, MRC has a good trade off in communication performance versus implementation complexity [13]. A log-likelihood function for MRC can be expressed as

$$\begin{aligned} LL(x) &= \log[p(Y_{n,k}^p | X_{n,k}) \times p(Y_{n,k}^w | X_{n,k})] \\ &= -\frac{|Y_{n,k}^p - H_{n,k}^p X_{n,k}|^2}{\sigma_p^2} - \frac{|Y_{n,k}^w - H_{n,k}^w X_{n,k}|^2}{\sigma_w^2} \end{aligned} \quad (3)$$

where σ_p^2 and σ_w^2 are Gaussian noise variances of powerline and wireless communications, respectively, as in [13], [14].

There are many assumptions that are taken for granted in theoretical work; however, in implementation, various techniques are to be employed to meet or relax the assumptions. And overall system performance depends on the employed techniques. A list of assumptions and approaches to realize or tackle each is described in Section IV.

III. TESTBED OVERVIEW

Smart grid wireless communication standards of IEEE 802.11ah and IEEE 802.15.4g and powerline communication standards of G3, PRIME and IEEE P1901.2 use OFDM. Even so, these standards do not share the same system parameter

TABLE I: Parameters for common baseband transceiver for simultaneous PLC and wireless communications

Parameter	Value
Sample rate	400 kHz
OFDM symbol size	256 samples
CP length	64 samples
Frame duration	variable
Frame rate	2.5 frames/s
Active subcarriers	36
Modulation scheme	BPSK / Differential BPSK

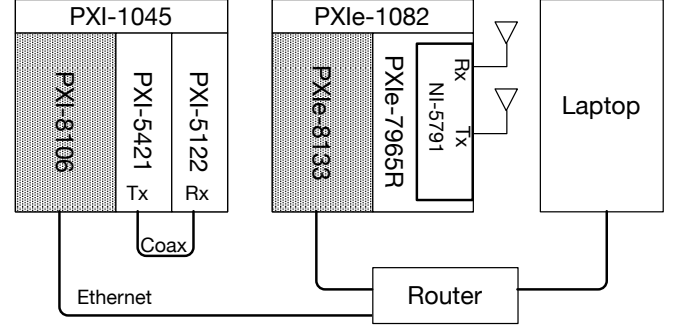


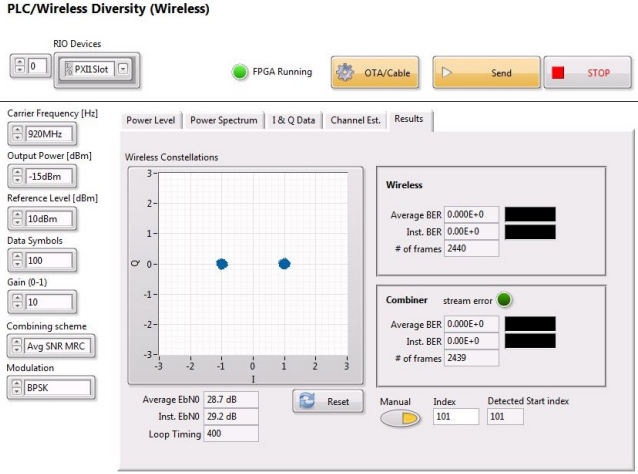
Fig. 2: Hardware Architecture

values. For the sake of simplicity, we use a common baseband transceiver for both wireless and powerline communications by using the parameters in Table I. Most parameters are chosen from IEEE P1901.2 [20]. A carrier frequency for wireless communications is set in the unlicensed 900 MHz band at 920 MHz.

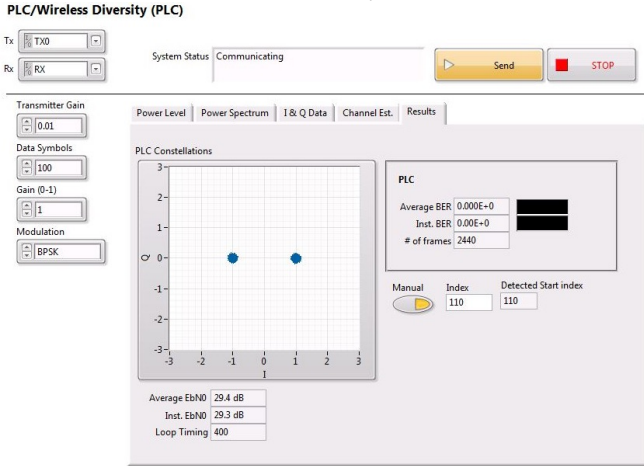
The purpose of the real-time PLC/wireless diversity testbed is to provide an environment for testing and evaluating various combining schemes under realistic conditions in real time. The testbed, thus, is able to gather received frames or decoded bits from both links for combining. It is also able to conduct separate frame decoding over each link to show improvement achieved with a combining scheme. An overview of the testbed platform is described in this section.

A. Hardware Architecture

The real-time testbed is built using products from National Instruments as shown in Fig. 2. Two chassis on the left and in the middle are for PLC and wireless communications, respectively. The two systems will be located in different places as they need different physical channels. Therefore the two communication systems reside in different chassis. A PXI chassis has slots that can accommodate an x86 controller and various modules. As Fig. 2 depicts, a PXI-1045 chassis on the left has a PXI-8106 controller, a PXI-5421 signal generator and a PXI-5122 digitizer. This chassis functions as a baseband PLC system. Similarly a PXIe-1082 chassis contains a PXIe-8133 controller, a PXIe-7965R FPGA module and an NI-5791 RF adapter module. Since the RF adapter module has both a transmit and a receive port, a unidirectional single-input single-output link can be established with a single adapter module.



(a) Wireless System



(b) PLC System

Fig. 3: Front Panels for the Testbed

The transmit and receive antennas for the wireless system are currently spaced about one meter apart to satisfy the far-field assumption. The transmit and receive ports in the PLC system are directly connected with a coaxial cable for testing purposes. These, however, are ready to be modified to meet research-specific demand. For example, the antennas can be placed where desired wireless interference exists, and the cable can be replaced with a powerline emulator or a real powerline.

The two controllers and a laptop computer are connected via an Ethernet router so that the laptop can act as a command center and a controller.

B. Software Architecture

The two controllers in the testbed run a real-time (RT) operating system (OS), and each RTOS runs its main program. The two independent systems have their own front panels as shown in Fig. 3 which displays controls and indicators of each communication system. The controller dedicated to the PLC system runs one thread performing frame generation, bit recovery, and transmission and reception of signals with

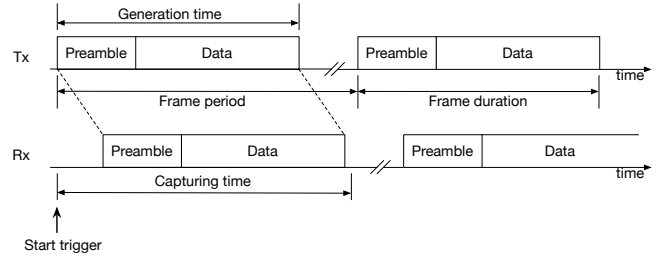


Fig. 4: Frame structure

hardware. The transmitter output signal can optionally bypass the hardware and be directly sent to a receive process in case one wants to test the transceiver without channels or with simulated channels. The other controller for the wireless system also performs the same process with different hardware. These threads are configured to iterate the whole process at the same rate which determines a frame period.

In addition, there is one more thread in the wireless system controller that carries out diversity combining. Log-likelihood ratios (LLRs) obtained from the PLC and wireless communication threads are forwarded to this thread along with a transmit bit sequence over first-in first-out (FIFO) queues and are processed in real time. It compares two transmit bit sequences to make sure the frames that it is trying to combine contain the same information, and then proceeds with combining.

C. Frame Structure

A frame consists of a variable number of OFDM symbols. Per the IEEE P1901.2 standard [20], the first nine symbols in a frame compose a preamble which is used for channel estimation, noise estimation and timing synchronization. The number of active subcarriers is 36 in the testbed as we consider transmission in the CENELEC A frequency band (35.9375 – 90.6250 kHz). The following OFDM symbols – data symbols – contain transmitted data on the same subcarriers as the preamble. BPSK or differential BPSK symbols made with a pseudo random bit sequence are mapped onto active subcarriers. The requested number of OFDM symbols compose the data part. Thus the frame has a variable length and is transmitted every 400 ms as shown in Fig. 4.

IV. TESTBED DESIGN AND IMPLEMENTATION CHALLENGES

Challenges in designing and implementing the testbed is equivalent to how to deal with assumptions that are posited in theory. Assumptions we take care of in this testbed implementation are listed in Table II along with a summary of realization approaches and sections for the details.

A. Channel and Noise Estimation

Channel and noise are intentionally generated in simulation. Hence one has direct access to parameters and instant realizations of channel and noise models and takes advantage of it. The testbed, however, has to estimate parameters to exploit

TABLE II: Realizing Assumptions in Communication Theory in the Testbed

Assumption	Realization	Section
A1. Channel knowledge	LS estimation	IV-A
A2. Noise variance knowledge	Estimation [21]	IV-A
A3. Sample timing detection	Peak detection or manual	IV-B
A4. Sampling frequency offset	Reference clock synch.	IV-C
A5. Carrier frequency offset	Local oscillator synch.	IV-C
A6. Frame transmission synch.	Deterministic OS	IV-D

them in signal processing. A preamble in a frame is used for such estimation.

As with other common OFDM communication systems, the testbed employs a frequency domain least square (LS) channel estimator. There are nine OFDM symbols in the preamble, and the channel estimates obtained from the those symbols are averaged in order to reduce the effects of noise. Channel estimation takes place once at the beginning of every frame, and the estimate is used to equalize data symbols in the same frame. For further improvement in estimation, additional pilots may be embedded within data symbols or other estimation techniques may be used.

Frequency domain zero forcing (ZF) channel equalization is then performed on data symbols with the obtained channel estimate, and data bits are recovered through symbol demapping. The testbed takes advantage of channel coding and employs the convolutional encoder along with the Viterbi decoder. The symbol demapper calculates the LLRs and sends them to the decoder of each system. At the same time, the LLRs are sent to the combining thread as well to perform diversity.

Noise variance and E_b/N_0 are estimated and averaged in real-time. The proposed noise variance estimation technique in [21] is useful when a preamble consists of more than one identical OFDM symbol such as one used in this testbed. Since a frame is assumed to be within a channel coherence time, $H_{n,k}$ and $H_{n+1,k}$ from (1) or (2) are to be identical. Plus, $X_{n,k}$ is known, and $Y_{n,k}$ is measured at receivers. Then, it is easy to obtain a power of $N_{n,k}$ by subtracting $Y'_{n,k}$ from $Y'_{n+1,k}$ where $Y'_{n,k} = Y_{n,k}/X_{n,k}$. An average of obtained power over frequency and time is manipulated to estimate a variance of noise as

$$\hat{\sigma}^2 = \frac{1}{2KN} \sum_{k=0}^{K-1} \sum_{n=0}^{N-1} \{|Y'_{n,k} - Y'_{n+1,k}|^2\}. \quad (4)$$

After estimating the noise variance, E_b/N_0 can be easily calculated.

B. Sample Timing Detection

Receivers in this testbed do not capture signals all the time, but start simultaneously with transmitters by the trigger and stop upon receiving the requested number of samples. A time of arrival of frame is unknown because of a propagation delay and a channel delay even if the transmitter and the receiver start simultaneously. For this reason, the receivers capture longer than the frame length as shown in Fig. 4. The receivers figure out a starting point of the received frame and place

the FFT window on the cyclic prefix (CP) boundary. Sample timing detection, thus, is one of the most important and the earliest processes on the receiver side. To find a starting point of a frame, peaks of cross correlation between a known OFDM symbol of preamble and a received preamble in a capture are detected and used.

Sample timing detection may not work correctly when the transmit power is too low. The testbed, therefore, provides an option to manually correct the timing. The timing offset remains unchanged as long as antenna distance or cable length does not change. Once a correct offset is obtained when the power is high enough, one can switch over to manual correction and use the obtained offset for low transmit power.

C. Sampling and Carrier Frequency Offsets

Offsets in sampling and carrier frequencies are commonly ignored in simulation as these are caused by separate oscillators in hardware. The offsets can be compensated with additional signal processing or canceled by synchronizing the oscillators. The testbed takes the synchronization approach since performance degradation due to additional signal processing can be avoided.

A transmitter and a receiver are synchronized in two ways. The PLC system synchronizes sample clocks of the transceiver to a reference clock generated in a backplane of a PXI chassis to prevent two sample clocks from drifting away. The transmitter also sends out a start trigger to the receiver to ensure they can start simultaneously. The wireless system employs the identical synchronization technique. Plus, a single local oscillator located in the adapter module is used by both an upconverter and a downconverter resulting in a zero carrier frequency offset.

D. Frame Transmission Synchronization

In order to prevent overflow of the FIFO queues in the combining thread, frame transmission of the two systems starts at the same time and transmission rates are the same. However, they operate independently without sharing any triggers or signals over a wire. The testbed, thus, takes advantage of the deterministic RTOS and uses a timed-loop in both the PLC and the wireless threads. The start, idle and stop flags are generated from the wireless system and are read by the PLC system over TCP/IP. This may introduce a delay up to several hundred milliseconds; however, once the systems start, they run at the same speed with a negligible jitter.

V. INITIAL RESULTS

A combining scheme of MRC is used in this section for testbed demonstration. As the log-likelihood function described in [14] indicates, the LLR computed with the MRC scheme is nothing but a sum of LLRs from both communications.

Two cases are taken into account for demonstration. In the first case, one of the links is in good shape so that all transmitted data can be recovered without an error while the other link is poor. We see that MRC can recover data even

TABLE III: Combiner Performance

(a) Wireless link is down

	PLC	Wireless	Combiner
E_b/N_0	7.30 dB	N/A	N/A
BER	0	5.00×10^{-1}	0

(b) PLC link is down

	PLC	Wireless	Combiner
E_b/N_0	N/A	8.56 dB	N/A
BER	5.00×10^{-1}	0	0

though one of the links is completely down. In the second case, E_b/N_0 for both systems is identical and is swept to plot BER curves. Or E_b/N_0 of one system, the wireless communication system in this case, is fixed and the other changes. We see that performance of MRC over physical channels is very comparable with simulation.

A. One link is down

In the first test case, one link is reliable, and the other is completely down, or equivalently, a transmitter does not generate a signal at all. This scenario sounds trivial, and results look obvious. However, it is a necessary test case to examine if one communication system can function as a backup for the other. With an MRC scheme, smart grid needs not physically switch over between powerline and wireless communications.

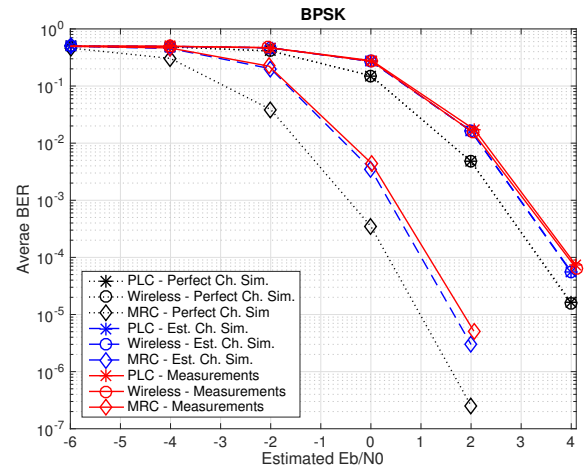
The testbed transmits more than 200,000 frames over physical channels to measure BERs of each case. When one of the channels is reliable enough, we can see from Table III that the combiner always yields zero BER proving that the MRC scheme can recover transmitted information even with the other channel completely down. It is quite an expected result, but we stress that it is demonstrated that diversity of heterogeneous communication technologies helps to build a more reliable smart grid communication system.

B. Bit error rate curves

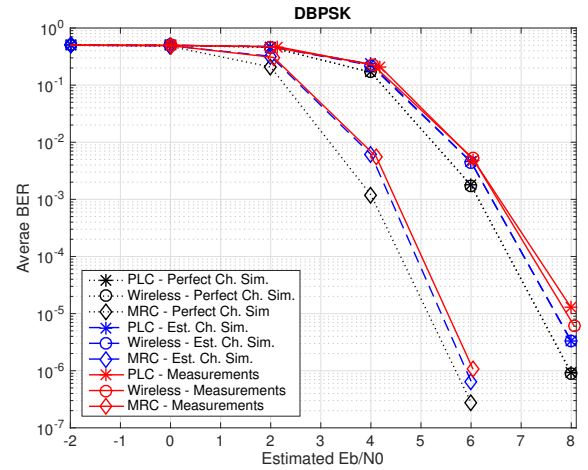
Performance of MRC measured on the testbed is compared with simulation by plotting BER curves. As shown in Fig. 5 and 6, we compare three sets of BER curves : 1) perfect channel simulation, 2) estimated channel simulation and 3) testbed measurements. Measurements made on the testbed are essentially based on channel estimation. In each set, there are three curves: PLC, wireless and combined.

Two sub-figures in Fig. 5 are obtained with different modulations: BPSK and differential BPSK. A set of curves from simulation with perfect channel is a baseline due to perfect channel knowledge known at the receiver. A set of measurement curves cannot achieve lower BER than the other sets because of employment of hardware as well as imperfect channel information. In both BPSK and differential BPSK cases, nevertheless, BER curves from measurements are very close to those from simulation using an estimated channel.

Focusing on the BPSK modulation shown in Fig. 5a, an E_b/N_0 gain obtained by MRC and perfect channel knowledge at BER of 10^{-4} is approximately 3 dB. At the same BER, the



(a) BPSK modulation



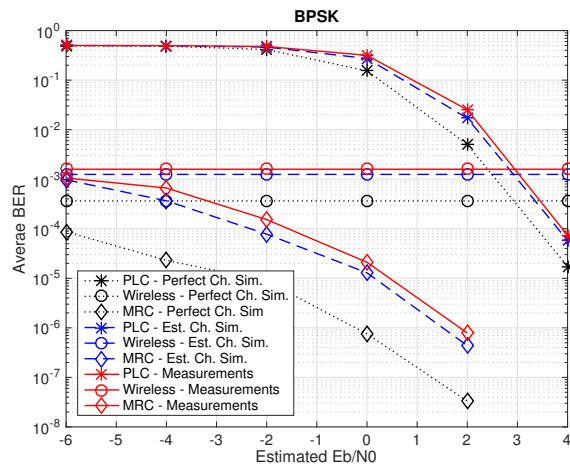
(b) Differential BPSK modulation

Fig. 5: BER vs. E_b/N_0 curves

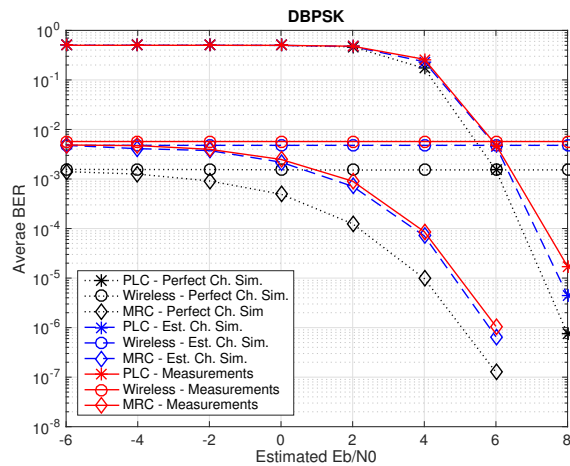
measured gain on the testbed is almost 3 dB as well. In other words, it is validated with the testbed that performance of MRC in simulation can closely be achieved in practice.

For differential BPSK shown in Fig. 5b, an E_b/N_0 loss due to imperfect channel information is smaller than the BPSK case. That is because differential BPSK modulation does not require a channel equalizer and is not affected by channel estimation. As with BPSK, the measurements show that almost the same E_b/N_0 gain is achievable as simulation. Note that E_b/N_0 ranges are different in two sub-figures in Fig. 5, and differential BPSK needs a higher E_b/N_0 than BPSK to achieve the same BER.

Fig. 6 shows BER curves as with Fig. 5, but E_b/N_0 for the wireless system is fixed at 3 dB and 6 dB for BPSK and differential BPSK, respectively. With both modulations, it is seen that MRC improves BER as E_b/N_0 of the PLC system increases. Improvement is prominent with low E_b/N_0 . In the E_b/N_0 range from -6 to -2 in Fig. 6a and -6 to 2 in Fig. 6b, BER of the PLC stays around 0.5; however, MRC still can



(a) BPSK modulation



(b) Differential BPSK modulation

Fig. 6: BER vs. E_b/N_0 curves with E_b/N_0 for wireless system fixed at (a) 3 dB with BPSK, and (b) 6 dB with differential BPSK

extract information from the poorly performing system and evidently suppresses BER. Fig. 6 can be alternatively interpreted that performance of the PLC alone can be drastically boosted with the help of the wireless system.

VI. CONCLUSION AND FUTURE WORK

In this paper, we propose implementation of a flexible real-time testbed for evaluation of diversity combining schemes over PLC and wireless communications. Detailed assumptions and approaches in designing and implementing the testbed are also provided. The testbed consists of powerline and wireless OFDM communication systems using the CENELEC A band and the unlicensed sub-1GHz band, respectively, and is ready to emulate a smart grid communication network. Similar transceiver processing is employed by the two systems and is flexible enough to be modified per research demand.

We demonstrated the testbed in two different scenarios with the combining scheme of MRC. It was first shown that

diversity makes smart grid communications more robust by recovering transmitted information even when one of two available links is completely down. We then plotted BER curves obtained from measurements and simulations to show that performance of MRC in practice is comparable with simulation in several test cases.

REFERENCES

- [1] National Energy Technology Laboratory, "Modern grid benefits," Aug. 2007.
- [2] U.S. Department of Energy, "The smart grid: An introduction," https://energy.gov/sites/prod/files/oeprdoc/DocumentsandMedia/DOE_SG_Book_Single_Pages.pdf, [Online; accessed Mar. 13, 2017].
- [3] "Monthly energy review," U.S. Energy Information Administration, Washington, DC, USA, Jul. 2016.
- [4] U.S. Energy Information Administration, "Preliminary monthly electric generator inventory," Jul. 2016.
- [5] U.S. Department of Energy, "Smart grid system report," Aug. 2014.
- [6] U.S. Energy Information Administration, "Smart grid legislative and regulatory policies and case studies," Dec. 2011.
- [7] H. Farhangi, "The path of the smart grid," *IEEE Power and Energy Magazine*, vol. 8, no. 1, pp. 18–28, Jan. 2010.
- [8] V. C. Gungor, B. Lu, and G. P. Hancke, "Opportunities and challenges of wireless sensor networks in smart grid," *IEEE Transactions on Industrial Electronics*, vol. 57, no. 10, pp. 3557–3564, Oct. 2010.
- [9] V. C. Gungor, D. Sahin, T. Kocak, S. Ergut, C. Buccella, C. Cecati, and G. P. Hancke, "Smart grid technologies: Communication technologies and standards," *IEEE Transactions on Industrial Informatics*, vol. 7, no. 4, pp. 529–539, Nov. 2011.
- [10] J. Zheng, D. W. Gao, and L. Lin, "Smart meters in smart grid: An overview," in *Proc. IEEE Green Technologies Conference*, Apr. 2013, pp. 57–64.
- [11] M. Nassar, J. Lin, Y. Mortazavi, A. Dabak, I. H. Kim, and B. L. Evans, "Local utility power line communications in the 3–500 kHz band: Channel impairments, noise, and standards," *IEEE Signal Processing Magazine*, vol. 29, no. 5, pp. 116–127, Sep. 2012.
- [12] M. Nassar, A. Dabak, I. H. Kim, T. Pande, and B. L. Evans, "Cyclostationary noise modeling in narrowband powerline communication for smart grid applications," in *Proc. IEEE International Conference on Acoustics, Speech and Signal Processing*, Mar. 2012, pp. 3089–3092.
- [13] S. W. Lai and G. G. Messier, "Using the wireless and PLC channels for diversity," *IEEE Transactions on Communications*, vol. 60, no. 12, pp. 3865–3875, Dec. 2012.
- [14] M. Sayed and N. Al-Dhahir, "Narrowband-PLC/wireless diversity for smart grid communications," in *Proc. IEEE Global Communications Conference*, Dec. 2014, pp. 2966–2971.
- [15] M. Mokhtar, W. U. Bajwa, M. Elgendedy, and N. Al-Dhahir, "Exploiting block sparsity for joint mitigation of asynchronous NBI and IN in hybrid powerline-wireless communications," in *Proc. IEEE International Conference on Smart Grid Communications*, Nov. 2015, pp. 362–367.
- [16] M. Sayed, G. Sebaali, B. L. Evans, and N. Al-Dhahir, "Efficient diversity technique for hybrid narrowband-powerline/wireless smart grid communications," in *Proc. IEEE International Conference on Smart Grid Communications*, Nov. 2015, pp. 1–6.
- [17] W. Tushar, C. Yuen, B. Chai, S. Huang, K. L. Wood, S. G. Kerk, and Z. Yang, "Smart grid testbed for demand focused energy management in end user environments," *IEEE Wireless Communications*, vol. 23, no. 6, pp. 70–80, Dec. 2016.
- [18] M. H. Cintuglu, O. A. Mohammed, K. Akkaya, and A. S. Uluagac, "A survey on smart grid cyber-physical system testbeds," *IEEE Communications Surveys Tutorials*, vol. 19, no. 1, pp. 446–464, Nov. 2016.
- [19] J. Sung and B. L. Evans, "Simultaneous powerline and wireless smart grid communications testbed," software Release, Mar. 29, 2017, <http://users.ece.utexas.edu/~bevans/projects/plc/software/testbed/>.
- [20] "IEEE P1901.2/D0.11.00 draft standard for low frequency (less than 500 kHz) narrow band power line communications for Smart Grid applications," *IEEE Standards Association*, Aug. 2013.
- [21] G. Ren, H. Zhang, and Y. Chang, "SNR estimation algorithm based on the preamble for OFDM systems in frequency selective channels," *IEEE Transactions on Communications*, vol. 57, no. 8, pp. 2230–2234, Aug. 2009.